

## Size effects in the optical properties of $\text{Au}_n\text{Ag}_n$ embedded clusters

E. Cottancin,\* J. Lermé, M. Gaudry, M. Pellarin, J.-L. Vialle, and M. Broyer

*Laboratoire de Spectrométrie Ionique et Moléculaire, Université Claude Bernard Lyon I, UMR CNRS 5579, 43. Boulevard du 11 Novembre 1918, 69 622 Villeurbanne Cedex, France*

B. Prével, M. Treilleux, and P. Mélinon

*Département de Physique des Matériaux, Université Claude Bernard Lyon I, UMR CNRS 5586, 43. Boulevard du 11 Novembre 1918, 69 622 Villeurbanne Cedex, France*

(Received 24 March 2000)

The optical properties of bimetallic silver-gold clusters are investigated in the size range 1.9–2.8 nm. Clusters, produced by laser vaporization of an alloy target Au-Ag (50%-50% atomic composition) are embedded with a low concentration in an alumina matrix. The mixed particles have the same stoichiometry as the rod. Absorption spectra exhibit a plasmon resonance band between those of pure Au and Ag embedded clusters, shifting towards higher energies with decreasing cluster size. Theoretical calculations in the frame of the time-dependent-local-density-approximation, including an inner skin of ineffective screening and the porosity of the matrix, are in good agreement with experimental results.

### I. INTRODUCTION

The optical properties of small metal particles,<sup>1</sup> used for many centuries in the art of making stained glass,<sup>2</sup> are a telltale sign of their electronic structure and have been thus extensively studied. The growing interest in the past decades in this field can be related to the prospective applications and to the extension of these studies to the nanosized domain. Indeed, the optical response in the range of the nanometer (dipolar approximation) depends crucially on the particle size due to quantum effects.

For metal particles, the surface-plasmon resonance, classically described as the collective oscillation of the conduction electrons subjected to an electromagnetic excitation, is the main feature of the optical response. Therefore, the photoabsorption spectrum is dominated by an absorption band whose position and width depend on the intrinsic properties of the clusters and on the surrounding medium. For alkali and noble metals, the surface plasmon occurs in the near ultraviolet-(UV) visible range.

In the case of free alkali clusters,<sup>3,4</sup> a redshift (shift towards lower energies) of the plasmon resonance with decreasing particle size is observed. This behavior is interpreted by the increasing influence of the spill-out effect for the small sizes.<sup>5</sup>

The interpretation of the optical properties of noble-metal clusters is a tickler because of  $d$ -core electron polarization.<sup>6–9</sup> For example, photoabsorption spectra of gold nanoparticles embedded in a transparent matrix reveal a blueshift (shift towards larger energies) with decreasing cluster size.<sup>10</sup> The size effects of free or embedded Ag and Au clusters (with a diameter lower than 5 nm) are now well-understood.<sup>11–13</sup> The quenching of the size effects in silver and the blueshift in gold are well reproduced by time-dependent-local-density-approximation (TDLDA) calculations taking into account the polarization of the  $d$ -core electrons in a two region dielectric model (the screening effects are less effective over a thin surface layer inside the metallic

particle) and the porosity of the matrix. The location of the Mie frequency relative to the maximum of the sharp peak in the real part of  $\epsilon_d(\omega)$  was found to be the key feature ruling the competition between the blueshift induced by the skin region of reduced polarizability and the redshift induced by the spill out.  $\epsilon_d(\omega)$  is the interband contribution in the dielectric function of the metal.

Since these size effects are well understood in pure metal particles, it becomes interesting to extend these studies to bimetallic clusters. The specific properties of alloys in metal physics lead to think that the elaboration of new original nanostructures can be achieved.

In the small size domain, depending on the production methods, bimetallic particles form either alloys (the two metals are homogeneously mixed at an atomic or nanometer level) or segregated systems: in this last case the second metal forms a mantle around a core made up of the first one. Many studies have been devoted to bimetallic systems by chemical ways. As an example, Ag or Au core particles coated with a second metal  $X$  ( $X = \text{Pb}, \text{Cd}, \text{In}, \text{Tl}, \text{Sn}$ ) have been produced.<sup>14–17</sup> Concerning the system Ag-Pt, alloyed or segregated particles have been produced by chemical ways.<sup>18,19</sup>

Pd-Pt clusters have been also produced by laser vaporization of an alloy target.<sup>20,21</sup> In this last case, ion-scattering spectroscopy and photoevaporation experiments show that the palladium is mainly on the surface. It comes out from these studies that the component having the smaller sublimation specific heat or surface energy, accumulates preferentially at the surface in order to minimize the total energy. A model, based on a tight-binding scheme,<sup>22</sup> developed by Rousset *et al.*, accounts well for the surface segregation in Pd-Pt.

Obviously this law has to be considered with caution for the systems in solutions like colloids for which the surface energies depend on the surrounding medium and on the surface adsorbed ions. Moreover all these chemical methods have also some drawbacks. The adjunction of various ele-

ments during the growth of the clusters may have some unexpected effects on the optical-absorption spectra. Mulvaney<sup>23</sup> reviews the different problems that can occur by these methods. For instance, electronic coupling with a solvent or chemisorption induce a shift of the plasmon resonance. However these methods remain the only ones allowing the formation of either alloyed or segregated particles.

Up to now, most of the optical investigations have been performed on the Au-Ag system in solution. By this way, one is able to make segregated or alloyed particles, at least for large clusters ( $\varnothing > 10$  nm).<sup>19,24</sup>

The first publication devoted to Au-Ag particles<sup>25</sup> compared the experimental optical spectrum with the Mie theory<sup>26</sup> assuming the segregation of Ag around a gold core. Later, Papavassilou<sup>27</sup> studied the incidence of the relative concentration of the two metals on the plasmon resonance in alloyed particles. He obtained a linear evolution of  $\lambda_p$  (wavelength of the surface plasmon) versus the Ag/Au stoichiometry for particles of mean diameter 10 nm. Sinzig *et al.*<sup>28</sup> studied theoretically and experimentally the optical properties of Au-Ag particles bigger than 10 nm in diameter and showed the differences between coated and alloyed systems. As a general rule, one resonance is observed for alloys, shifting from the Ag Mie frequency to the Au one with the Ag/Au composition whereas more complex and broader structures are observed in the case of coated systems.

In the last ten years the optical properties of Au-Ag particles have been more systematically studied by Link *et al.*<sup>29</sup> Experiments on alloyed particles of around 10 nm in diameter exhibit a linear shift towards shorter wavelengths of  $\lambda_p$  with increasing concentration of silver, in agreement with the results of Papavassiliou but in disagreement with those of Teo, Keating, and Kao<sup>30</sup> who obtain a strongly nonlinear evolution. These differences emphasize that the optical properties depend crucially on the nanostructure (alloy, stacking of nanodomains or coated particles) of bimetallic particles.

Up to now all the experiments show the differences between alloys and coated systems for different relative concentrations of the two metals for particles larger than 5 nm in diameter but the size effects have not been systematically investigated. On a theoretical point of view, the interpretation of optical spectra is less easy because the effective dielectric function of the composite particles depends strongly on their structure at an atomic scale. We can also underline that the Mie theory is not necessarily suitable for very small particles for which quantum corrections are expected.

Our study intends to probe smaller particles (diameter  $\varnothing < 5$  nm) and to evaluate the size effects in the optical properties of alumina-embedded mixed clusters Au-Ag produced by laser vaporization of an alloy target Ag-Au (50%-50% at %). Such works are near our earlier ones on pure Ag or Au clusters.<sup>10,12,13</sup> The optical spectra exhibit an absorption band whose characteristics are intermediate between those of pure gold and pure silver embedded clusters. The other feature emerging from the absorption measurements is the blueshift of the plasmon resonance with decreasing cluster radius. Our results are analyzed through TDLDA calculations, in the frame of an improved formalism.<sup>31</sup> The interpretation rests on a common hypothesis concerning the effective dielectric function of the composite particles, which consists in taking

the composition average of the dielectric functions of both metals.

The plan of the paper is as follows. Section II A briefly recalls the sample production and characterizations. We then provide in Sec. II B the experimental results. The comparison with TDLDA calculations are given in Sec. III.

## II. EXPERIMENTS

### A. Sample preparation and characterizations

Clusters are produced by a laser vaporization source described in previous papers.<sup>10,32</sup> In a small chamber under a continuous flow of helium (few tens of mbar), a rod of a gold-silver alloy Au-Ag (50%-50% in atomic concentration) is vaporized by a frequency-doubled Nd-yttrium-aluminum garnet (YAG) pulsed laser ( $\lambda = 532$  nm). The so-formed atomic plasma, cooled by the helium gas, expands through a nozzle and combines into clusters. This continuous helium flow allows a good stability of the cluster deposition rate. Moreover, the helium pressure is the key to controlling the size of the free clusters and thus the size distribution in the samples.

The clusters, collimated through a skimmer, pass next into the high-vacuum deposition chamber ( $10^{-7}$  mbar). Finally, the clusters and the transparent dielectric matrix are codeposited on a substrate whose kind depends on further measurements to be performed. Clusters and matrix deposition rates are measured by two quartz balances which allow setting the film thickness and the volumic fraction of metal in our samples. In order to avoid any cluster coalescence, the metal concentration is chosen to lie below 5%. The characteristics of the pure alumina matrix films, described elsewhere,<sup>10</sup> were analyzed through various techniques. Briefly, the alumina matrix has an amorphous structure with an important porosity (45% compared to crystalline  $\text{Al}_2\text{O}_3$ ) and Rutherford-back-scattering (RBS) measurements show a slight overstoichiometry according to the raw formula  $\text{Al}_2\text{O}_{3.2}$ .

Energy-dispersive x-ray and RBS analysis confirm the low-volumic concentration of metal in our samples. Besides, the relative atomic fraction 50%–50% is found again in our samples, suggesting that the stoichiometry inside the clusters is the same as in the alloy rod. The transmission electron microscopy (TEM) micrographs reveal almost spherical clusters randomly distributed in the transparent matrix (Fig. 1). Size distributions are deduced from the micrographs over a population of 750 to 1500 particles per sample. The mean diameter  $\langle D \rangle$  is from sample *a* to *c*: 1.9, 2.2, and 2.8 nm (Fig. 1) while the concentrations are between 2.5% and 5%. One can notice that the larger clusters (sample *c*) are produced by using a mixing of helium and argon in the source chamber.

### B. Optical-absorption measurements

Absorption measurements are performed with a Perkin-Elmer spectrophotometer on the films deposited on pure silica (suprasil) substrates, in a spectral range 180–800 nm (1.55–6.89 eV). Results are displayed in Fig. 2(a) for  $\text{Au}_n$ ,  $(\text{Au}_{0.5}\text{Ag}_{0.5})_n$  and  $\text{Ag}_n$  particles embedded in an alumina matrix, produced via the same technique. The three spectra exhibit an absorption band attributed to the surface-plasmon

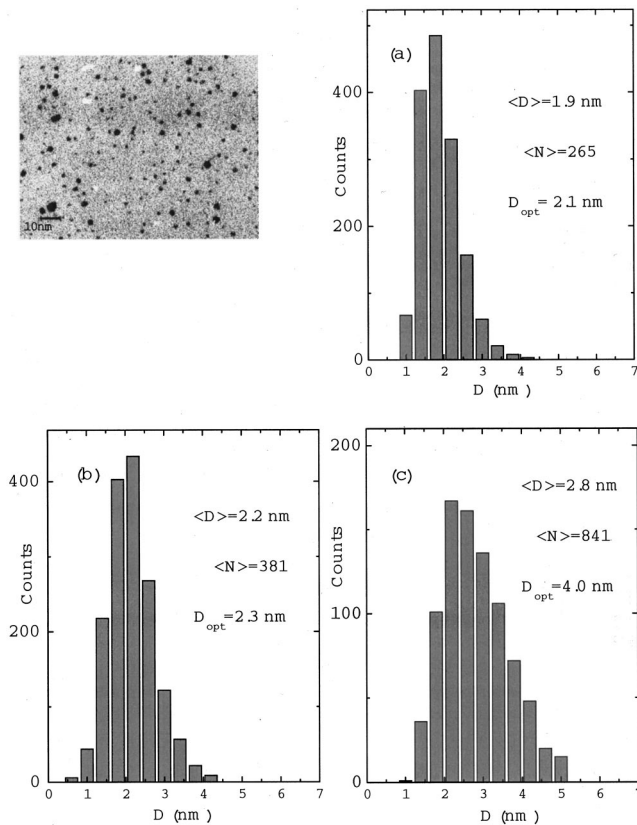


FIG. 1. Size distributions deduced from TEM micrographs for three different samples (a), (b), and (c).  $\langle D \rangle$  denotes the mean diameter and  $\langle N \rangle$  the corresponding mean number of atoms per cluster.  $D_{\text{opt}}$  designs the optical diameter, defined as  $\langle D^3 \rangle^{1/3}$ . The film thickness is around 150 Å and the metal concentration is 2.5%, 3.5%, and 5% for the samples (a), (b), and (c), respectively. As an illustration the TEM micrograph of the sample (a) is displayed.

resonance and an increasing absorption in the UV region, due to interband transitions, proper to noble metals. The general features of these spectra are similar; the main differences lie in the position of the plasmon resonance occurring, respectively, for  $\text{Au}_n$ ,  $(\text{Au}_{0.5}\text{Ag}_{0.5})_n$  and  $\text{Ag}_n$  at 2.40, 2.56, and 2.9 eV and its damping. The disparities in the overall absorption efficiency result from different quantities of metal in our samples (various thickness and metal volumic concentrations). The resonance in the case of  $(\text{Au}_{0.5}\text{Ag}_{0.5})_n$  clusters occurs almost halfway between those of pure gold and pure silver embedded clusters. The shape of the spectrum suggests that gold and silver are not segregated in the cluster if one compares with the absorption spectra of alloyed and segregated Au-Ag clusters in the literature,<sup>27,28,30</sup> but as yet no similar experiments have been performed on so small clusters ( $\varnothing < 5 \text{ nm}$ ). Moreover the tendency of these two materials for alloying in many cases<sup>19,24</sup> and our production method strengthen this assumption (high-cooling rate in the source).

The second study is focused on the size effects in the optical response. Figure 2(b) displays the absorption spectra for different samples with the size distributions presented in Fig. 1 ( $1.9 \text{ nm} < \langle D \rangle < 2.8 \text{ nm}$ ). The observed blueshift of the resonance with decreasing cluster size is intermediate between the size evolution obtained in pure  $\text{Ag}_n$  and  $\text{Au}_n$  clusters. For  $\text{Ag}_n$  clusters the size effects are almost completely

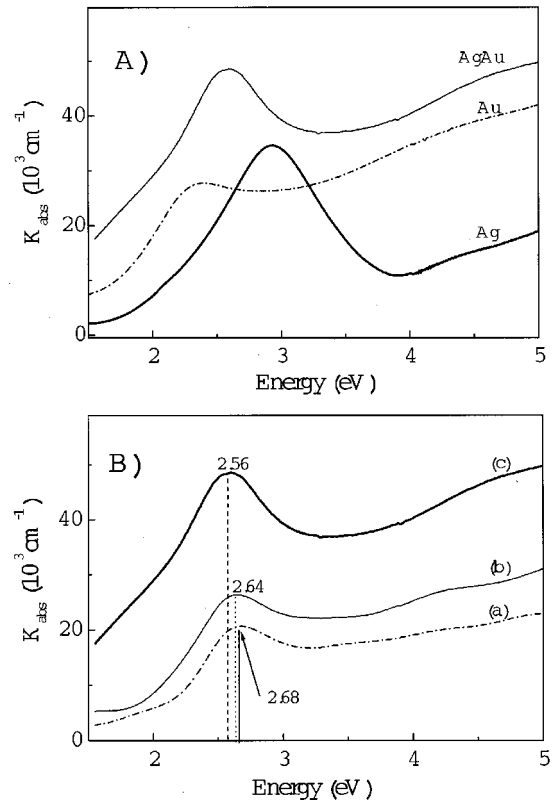


FIG. 2. (a) Absorption coefficient versus energy of alumina embedded particles of  $\text{Au}_n$ ,  $(\text{Au}_{0.5}\text{Ag}_{0.5})_n$ , and  $\text{Ag}_n$  clusters with respective mean diameter:  $\langle D \rangle = 2.7, 2.8$ , and  $3.1 \text{ nm}$ ; (b) Absorption coefficient versus energy of three different samples of alumina embedded  $(\text{Au}_{0.5}\text{Ag}_{0.5})_n$  clusters whose mean diameter is 1.9, 2.2, and 2.8 nm for samples labeled (a), (b), and (c).

quenched when the Au cluster resonance exhibits a noticeable blueshift.<sup>10,13</sup> In addition to the damping due to the coupling between intra- and interband transitions, inhomogeneous effects are responsible for the large width of the plasmon resonance, namely, size, shape, and local porosity distributions in our samples.

A quantum approach is necessary to interpret these size effects since in this size range, the Mie theory is not relevant. The main difficulty is to evaluate the dielectric function of the mixed system Au-Ag.

### III. THEORY AND DISCUSSION

Calculations based on the TDLDA formalism within the framework of a mixed classical/quantal model have been performed and the size evolution of the Mie band location compared with the experimental findings. The ingredients of the model calculations have been extensively discussed in previous papers,<sup>10,12,13</sup> and will be reminded only briefly for the reader information. The ionic metal background is phenomenologically described by both: (i) a step-walled homogeneous spherical charge distribution (jellium) of radius  $R = r_s N^{1/3}$  ( $r_s$  is the so-called Wigner-Seitz radius characterizing the conduction electron density in the bulk material), and, (ii) a homogeneous dielectric medium [dielectric function  $\epsilon_d(\omega)$ ] extending up to  $R_1 = R - d$  where  $d$  is the thickness of the inner skin of ineffective screening<sup>33,34</sup> (intrinsic parameter of the cluster). Moreover, due to the local porosity



at the metal-matrix interface, resulting from the surface roughness, as well as the experimental codeposition technique used, a vacuum rind of thickness  $d_m$  (“extrinsic” parameter) is introduced in the model. Namely, the alumina matrix [dielectric function  $\varepsilon_m(\omega)$ ] extends only beyond the interface  $R_2 = R + d_m$ . The relevance of both model ingredients for interpreting the absorption spectra of free and matrix-embedded noble-metal clusters was emphasized and discussed in our works on  $\text{Al}_2\text{O}_3$ -embedded  $\text{Au}_N$  and  $\text{Ag}_N$  clusters.<sup>10,12,13</sup> Since the composite  $\text{Au-Ag}:\text{Al}_2\text{O}_3$  samples have been elaborated under the same experimental deposition conditions as those prevailing in our previous works, the same parameter values have been used in the present calculations, namely,  $d(\text{Au-Ag}) = d(\text{Ag}) = d(\text{Au}) = 3.5$  a.u. and  $d_m = 2$  a.u. With regard to the theoretical framework, we remind that only the valence electrons are quantum mechanically described within the TDLDA formalism, when the optical response of both the ionic background and the surrounding matrix are phenomenologically described through their respective dielectric functions, assumed bulk-like. Unlike our previous works on  $\text{Ag}_N$  and  $\text{Au}_N$  clusters, the calculations reported in this paper have been carried out within a recently developed formalism that includes the interband transitions and self-consistently describes the mutual interplay between the optical excitations of the various media.<sup>31</sup> The implicit assumption concerning the size independence of  $\varepsilon_d(\omega)$  (input data of the model) could be called into question. Actually this hypothesis seems to be supported by photoelectron experiments on small noble-metal clusters<sup>35</sup> and ellipsometry measurements on  $\text{Au}_N:\text{Al}_2\text{O}_3$  films having various size distributions.<sup>10</sup> This shortcoming is thus expected to alter only slightly the theoretical results, all the more that most of the cluster sizes involved in this paper are sufficiently large to disregard the size effects in the  $d$ -band structure.

The central point to be tackled now is to estimate—at least approximately—the dielectric function related to the ionic cores in the bimetallic cluster. The problem of the determination of the effective dielectric function  $\varepsilon_{\text{eff}}$  of a composite material has a long history and research on this subject is currently active.<sup>36–38</sup> To our knowledge, except for obvious cases (i.e., simple geometries), and rigorous bounds derived from formal theoretical developments, accurate quantitative results are rather scarce. Actually the difficulty stems from the fact that such a quantity is, in addition to the volumic composition, dependent on the detailed micro(nano)structure of the heterogeneities, especially the relative spatial distributions of both constituents. The nanoscaled inner geometry cannot be determined but one can infer that no surface segregation (coated clusters consisting of a gold core with a silver shell or vice versa) occurs in the bimetallic  $(\text{Au}_x\text{Ag}_{1-x})_n$  clusters produced from the ablation of the fine-grained alloy rod, owing to both: (i) the propensity of these two metals of similar atomic and bulk properties ( $r_s \approx 3$  a.u., effective electron mass  $m \approx 1$ ) for alloying at any relative concentration  $x$  ( $0 \leq x \leq 1$ ), and, (ii) the high-cooling rate of the laser vaporization source. We can therefore reasonably assume that the very most of the clusters emerging from the source—and subsequently embedded in the alumina matrix—keep memory of the statistical sticking processes during the growing stage, namely, are globally homoge-

neous. This homogeneity is indeed a necessary prerequisite for defining an effective dielectric function for the metallic mixture.

In the present investigation we assume a very simple model, which has been invoked in numerous experimental works on colloidal mixed nanoparticles grown by electrochemistry in aqueous or organic solvents.<sup>29,30</sup> In this rough model the dielectric function of a metallic compound  $\text{A}_x\text{B}_{(1-x)}$  is given by the composition-weighted average of the dielectric functions characterizing the pure materials, i.e.,  $\varepsilon_{\text{av}}(\text{A}_x\text{B}_{1-x}) = \varepsilon(x') = x'\varepsilon(A) + (1-x')\varepsilon(B)$ , where  $x'$  is the volumic composition  $\{x' = x[r_s(A)/r_s(B)]^3\}$ . However it is worthwhile pointing out that the use of this simple ansatz for interpreting the experimental data seems to have been dictated only for numerical convenience and the lack of available alternate models. Nevertheless, the suitability of the above composition-weighted law for our samples can be qualitatively supported, under certain conditions. The first hypothesis, common to any composite medium models, grounds the possibility of expressing the effective dielectric function of the mixture in terms of those of its constituents: the cluster is assumed to contain homogeneous domains with dielectric constants equal—or at least close to—those of both pure materials  $A$  and  $B$ . The popular effective medium theories, as the Maxwell-Garnett<sup>39</sup> and Bruggeman<sup>40</sup> models, do not seem appropriate, for they explicitly assume particular domain shapes, namely, involve spherical inclusions embedded in, either the most abundant material (host medium), or the effective medium itself. Actually, since the value  $x = 0.5$  is far above the percolation threshold ( $\approx 0.25$ ), such a picture for describing our bimetallic clusters is irrelevant, even if the effective dielectric constants calculated within these two models could provide reasonable numerical estimates. A general formula, suitable for any kind of heterogeneity was derived 50 years ago.<sup>41</sup> In this formula the effective dielectric constant is expressed as a series expansion of the dielectric contrast parameter  $\delta\varepsilon = \varepsilon(A) - \varepsilon(B)$  whose coefficients depend on the volumic fraction  $x'$  and the statistical properties of the spatial distributions of both components  $A$  and  $B$ . Retaining only the three leading terms, the formula is

$$\begin{aligned} \frac{\varepsilon_{\text{eff}}(x')}{\varepsilon_{\text{av}}(x')} = & 1 - \frac{1}{3}x'y' \left( \frac{\delta\varepsilon}{\varepsilon_{\text{av}}(x')} \right)^2 \\ & + \left[ -\frac{2}{9}x'y'(x'-y') + (x'^2\lambda - y'^2\mu) \right] \\ & \times \left( \frac{\delta\varepsilon}{\varepsilon_{\text{av}}(x')} \right)^3 + \dots, \end{aligned} \quad (1)$$

where  $y' = 1 - x'$ , and  $\lambda$  and  $\mu$  are numerical parameters depending on the statistical spatial distributions of materials  $A$  and  $B$ , respectively. In the present case, since  $x' \approx 0.5$  ( $r_s = 3.01$  a.u. and  $3.02$  a.u. for gold and silver, respectively), and assuming identical statistical distributions for both metals ( $\lambda = \mu$ ), the third term in the series expansion vanishes. Assuming that the higher-order terms are negligible, to a very good accuracy one obtains:

$$\varepsilon_{\text{eff}}(x'=0.5) = \varepsilon_{\text{av}}(x'=0.5) \left[ 1 - \frac{1}{12} \left( \frac{\delta\varepsilon}{\varepsilon_{\text{av}}(x'=0.5)} \right)^2 \right]. \quad (2)$$

It is worthwhile noting that the above corrective term in  $\delta\varepsilon^2$  is consistent with the formula—found in many textbook on the subject—derived for a composite material having a very low-dielectric contrast parameter.<sup>42</sup> In addition, using the experimental data of the dielectric constants of bulk gold and silver,<sup>43</sup> we have checked that the real and imaginary components of the corrective term  $-(1/12)(\delta\varepsilon/\varepsilon_{\text{av}})^2$  are rather low, over the entire spectral range. Both values are close to zero below 2.4 eV and above 4 eV, but are strongly  $\omega$  dependent and larger between 2.7 and 3.7 eV, without however exceeding 0.22 (the interband contribution are mainly responsible for these features). Thus, as a first approximation, the simple composition-weighted average  $\varepsilon_{\text{eff}} \approx \varepsilon_{\text{av}}$  with  $x'=0.5$  is a suitable ansatz. Moreover, since gold and silver have almost identical bulk parameters  $r_s$  and  $m$ , and consequently a similar Drude contribution (intra-band contribution in the dielectric function), we have assumed that the dielectric function of the ionic background in the bimetallic clusters [ $\varepsilon_d(\omega)$ , input data in the TDLDA calculations] is the composition-weighted average of those of the two pure metals, previously determined by a Kramers-Kronig analysis.<sup>12,13</sup> In fact, the dielectric functions obtained by applying other effective medium formula (Maxwell-Garnett or Bruggeman) are very similar to the one derived presently (whatever the volumic fraction  $x'$  of the Au-Ag system is).<sup>44,45</sup> Results obtained when correction to the present simple ansatz  $\varepsilon_{\text{eff}} \approx \varepsilon_{\text{av}}$  is included, as well as those from a more realistic model for describing Au-Ag alloys at the atomic scale (compound material that cannot be pictured as a stacking of homogeneous domains *A* and *B*), will be reported in a forthcoming paper.

Figures 3(a) and 3(b) compared to Fig. 2 show that the experimental data are qualitatively well reproduced by the theory, on the one hand with respect to the differences in the absorption spectra between the three metals, Au, Ag, and Au-Ag, on the other hand with respect to the size evolution of the Mie band. Obviously perfect quantitative agreement between theory and experiment cannot be achieved owing to the large size-, shape-, and local-porosity-distributions in the samples, which lead to an *inhomogeneous* broadening and damping of the spectra. With respect to the size evolution of the peak plasmon maximum, the quantitative agreement is very good, but has to be considered as lucky (see below), in view of the crudeness of the model for  $\varepsilon_d$  in the mixed particles. Nevertheless, the order of magnitude of the rate of the peak plasmon shift versus size, intermediate between pure gold (noticeable blueshift trend as the size decreases) and pure silver (almost perfect quenching of finite-size effects) is well estimated. Figures 4(a) and 4(b) summarize the theoretical results, with regard to the peak plasmon maximum. Let us emphasize that, for consistency, the calculations for pure gold and silver clusters have been carried out with the same new formalism as used for the bimetallic clusters.<sup>46</sup> In addition, owing to the rather tiny size effects, a fine energy increment  $\Delta\omega$  has been used over the Mie band spectral range in order to unambiguously determine the size trend. When a single interface is involved (standard Mie theory) no

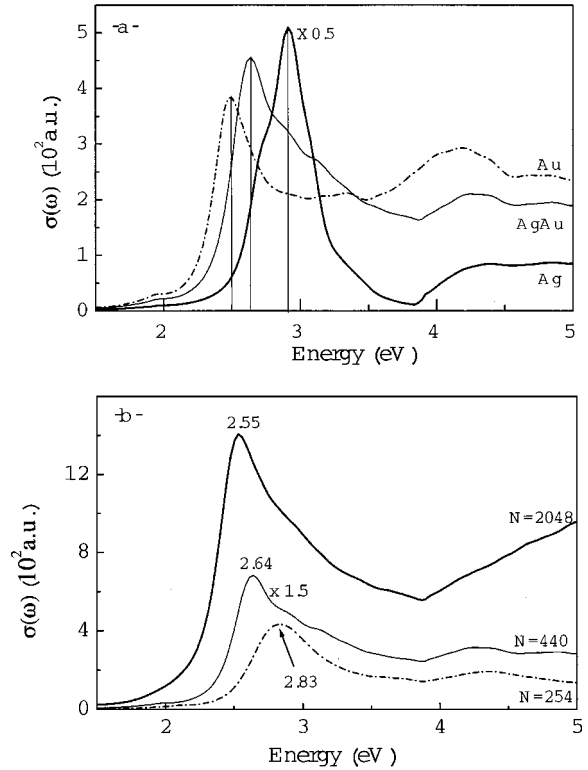


FIG. 3. (a) Theoretical absorption spectra of gold, silver, and mixed silver-gold clusters in an alumina matrix, calculated for  $N = 440$  atoms per cluster. The curve for Ag has been multiplied by a factor 0.5; (b) Theoretical absorption spectra of  $(\text{Au}_{0.5}\text{Ag}_{0.5})_n$  clusters in an alumina matrix for three different sizes. For the legibility the curve for  $N=440$  has been multiplied by a factor 1.5. The energy increment  $\Delta\omega$  is 0.03 eV and around the plasmon peak is divided by 10 for a better determination of the maximum.

size effects occur in the dipolar regime ( $\lambda \gg R$ ), except for a mere volume scaling factor. When the surface skins (thickness  $d$  and  $d_m$ ) of ineffective screening are included in the embedded-cluster model, finite-size effects result, but these are noticeably different from those calculated within the TDLDA-based quantum model [Fig. 4(a)]. This discrepancy stems from the large value of the Fermi wavelength  $\lambda_F \approx 3.3r_s$  relative to  $d$  and  $d_m$ . In Figs. 4(a) and 4(b) the comparison with experiment has been achieved by attributing to the experimental Mie-band maximum the size corresponding to the mean “optical diameter,” defined as  $\langle D^3 \rangle^{1/3}$  (black circles). The larger discrepancy between TDLDA theory and experiment for the smaller mean size for mixed clusters is maybe due to the fact that, around and above  $E=2.7$  eV, the corrective term in Eq. (2) is positive and rather large ( $\approx 0.17$ ), and consequently the theoretical results are slightly overestimated in the small size range.

The noticeable differences observed between theory and experiment for large  $\text{Ag}_n$  clusters deserve to be commented. For very large clusters the effects of the spill out and the surface skins of ineffective screening (thickness  $d$  and  $d_m$ ) vanish and the results tend obviously towards the predictions obtained by standard classical Mie calculations (a single metal/matrix interface). In the experiment the asymptotic values correspond to a metal sphere embedded in a porous alumina matrix. Taking into account the experimentally-determined dielectric function of our pure alumina films one

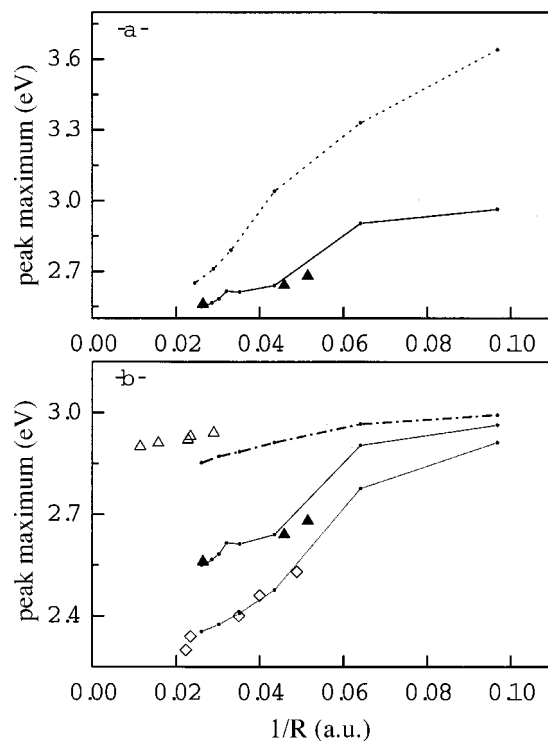


FIG. 4. The size evolution of the peak plasmon maximum within different models for particles embedded in an alumina matrix. (a) Classical results for  $(\text{Au}_{0.5}\text{Ag}_{0.5})_n$  clusters (dots); (a) and (b) TDLDA results (solid line) and experimental results (black triangles) for  $(\text{Au}_{0.5}\text{Ag}_{0.5})_n$  clusters; (b) TDLDA results (dashed line) and experimental results (open triangles) for  $\text{Ag}_n$  clusters; TDLDA results (dotted line) and experimental results (open rhomb) for  $\text{Au}_n$  clusters.

obtains the peak maximum values 2.89, 2.5, and 2.3 eV for  $\text{Ag}_n$ ,  $(\text{Au}_{0.5}\text{Ag}_{0.5})_n$ , and  $\text{Au}_n$  clusters, respectively. In the theoretical model the bulk alumina dielectric function is assumed beyond  $R_2$ . Therefore the theoretical asymptotic values correspond to a metal sphere embedded in bulk alumina, and are found to be 2.75, 2.43, and 2.25 eV, respectively. Refinement of the model by taking the dielectric function of the porous alumina matrix would increase slightly the theo-

retical results, and especially would correct the asymptotic size evolution for  $\text{Ag}_n$  clusters. This suggests that the model slightly overestimates the surface plasmon-frequency of mixed  $(\text{Au}_{0.5}\text{Ag}_{0.5})_n$  clusters. Our qualitative analysis remains however quite suitable.

In conclusion, despite the crudeness of the present hypothesis concerning the dielectric function  $\epsilon_d(\omega)$  of the composite ionic background, the agreement between theory and experiment seems to support the multi-interface model previously introduced for interpreting the optical response of matrix-embedded noble-metal particles. More conclusive information is expected to be provided by varying the relative metal composition  $x$  in the  $(\text{Au}_x\text{Ag}_{1-x})_n$  clusters (work in progress).

#### IV. CONCLUSION

Optical properties of mixed particles  $(\text{Au}_{0.5}\text{Ag}_{0.5})_n$  appear intermediate between those of pure  $\text{Au}_n$  and  $\text{Ag}_n$  clusters. On the one hand the plasmon resonance occurs halfway between the resonance in pure gold and silver particles, on the other hand the blueshift of the plasmon peak with decreasing cluster size is smaller than the blueshift in gold. The facility of these two materials for alloying and the production technique leads one to think that gold and silver are not segregated inside the particles.

The calculations based on the TDLDA formalism are found to be in good agreement with the experimental results in spite of the rough model used for evaluating the dielectric function of the ionic background in the bimetallic system.

Comparison with gold-silver clusters of various relative compositions would significantly advance the understanding of these mixed particles in this size range. The possibility of making segregated materials with a specifically designed vaporization source (with two rods) would allow to compare segregated and alloyed systems in a size range scarcely explored. In our laboratory, current research is directed towards this way.

#### ACKNOWLEDGMENTS

We wish to thank O. Boisson, C. Clavier, G. Guiraud, and F. Valadier for valuable technical assistance.

\*Email: cottanci@lasim.univ-lyon1.fr

<sup>1</sup>U. Kreibig and M. Vollmer, *Optical Properties of Metal Clusters* (Springer, Berlin, 1995).

<sup>2</sup>J. C. Valmalette, L. Lemaire, G. L. Hornyak, J. Dutta, and H. Hofmann, *Anal. Mag.* **24**, M23 (1996).

<sup>3</sup>J. Blanc, V. Bonacic-Koutecky, M. Broyer, J. Chevalere, P. Dugourd, J. Koutecky, C. Scheuch, J. P. Wolf, and L. Wöste, *J. Chem. Phys.* **96**, 1793 (1992).

<sup>4</sup>C. Bréchnac, P. Cahuzac, N. Kebaili, J. Leygnier, and A. Sarfati, *Phys. Rev. Lett.* **68**, 3916 (1992).

<sup>5</sup>V. V. Kresin, *Phys. Rep.* **220**, 1 (1992).

<sup>6</sup>J. Tiggesbäumker, L. Köller, H. O. Lutz, and K. H. Meiwes-Broer, *Chem. Phys. Lett.* **190**, 42 (1992).

<sup>7</sup>J. Tiggesbäumker, L. Köller, K. H. Meiwes-Broer, and A. Liebisch, *Phys. Rev. A* **48**, R1749 (1993).

<sup>8</sup>S. Fedrigo, W. Harbich, and J. Buttet, *Phys. Rev. B* **47**, 10 706 (1993).

<sup>9</sup>M. M. Alvarez, J. T. Khoury, T. G. Schaaff, M. N. Shafiqullin, I. Vezmar, and R. L. Whetten, *J. Phys. Chem. B* **101**, 3706 (1997).

<sup>10</sup>B. Palpant, B. Prével, J. Lermé, E. Cottancin, M. Pellarin, M. Treilleux, A. Perez, J. L. Vialle, and M. Broyer, *Phys. Rev. B* **57**(3), 1963 (1998).

<sup>11</sup>L. Serra and A. Rubio, *Z. Phys. D* **40**, 262 (1997).

<sup>12</sup>J. Lermé, B. Palpant, B. Prével, E. Cottancin, M. Pellarin, M. Treilleux, J. L. Vialle, A. Perez, and M. Broyer, *Eur. Phys. J. D* **4**, 95 (1998).

<sup>13</sup>J. Lermé, B. Palpant, B. Prével, M. Pellarin, M. Treilleux, J. L. Vialle, A. Perez, and M. Broyer, *Phys. Rev. Lett.* **80**, 5105 (1998).

<sup>14</sup>A. Henglein, *J. Phys. Chem.* **83**, 2858 (1979).

<sup>15</sup>A. Henglein, P. Mulvaney, T. Linnert, and A. Holzwarth, *J. Phys. Chem.* **96**, 2411 (1992).

<sup>16</sup>A. Henglein, P. Mulvaney, A. Holzwarth, and T. E. Sosebee, *Ber. Bunsenges. Phys. Chem.* **96**, 754 (1992).

- <sup>17</sup>A. Henglein and M. Giersig, *J. Phys. Chem.* **98**, 6931 (1994).
- <sup>18</sup>K. Torigoe, Y. Nakajima, and K. Esumi, *J. Phys. Chem.* **97**, 8304 (1993).
- <sup>19</sup>L. M. Liz-Marzan and A. P. Philipse, *J. Phys. Chem.* **99**, 15 120 (1995).
- <sup>20</sup>J. L. Rousset, A. M. Cadrot, F. S. Aires, A. Renouprez, P. Mélinon, A. Perez, M. Pellarin, J. L. Vialle, and M. Broyer, *Surf. Rev. Lett.* **3**, 1171 (1996).
- <sup>21</sup>J. L. Rousset, A. Renouprez, and A. M. Cadrot, *Phys. Rev. B* **58**, 2150 (1998).
- <sup>22</sup>J. L. Rousset, J. C. Bertolini, and P. Miegge, *Phys. Rev. B* **53**, 4947 (1996).
- <sup>23</sup>P. Mulvaney, *Langmuir* **12**, 788 (1996).
- <sup>24</sup>P. Mulvaney, M. Giersig, and A. Henglein, *J. Phys. Chem.* **97**, 7061 (1993).
- <sup>25</sup>R. H. Morriss and L. F. Collins, *J. Chem. Phys.* **41**, 3357 (1964).
- <sup>26</sup>A. L. Aden and M. Kerker, *J. Appl. Phys.* **22**, 1242 (1951).
- <sup>27</sup>G. C. Papavassiliou, *J. Phys. F* **6**, L103 (1976).
- <sup>28</sup>J. Sinzig, U. Radtke, M. Quinten, and U. Kreibitz, *Z. Phys. D* **26**, 242 (1993).
- <sup>29</sup>S. Link, Z. L. Wang, and M. A. El-Sayed, *J. Phys. Chem.* **103**, 3529 (1999).
- <sup>30</sup>B. K. Teo, K. Keating, and Y. H. Kao, *J. Am. Chem. Soc.* **109**, 3494 (1987).
- <sup>31</sup>J. Lermé, B. Palpant, E. Cottancin, M. Pellarin, B. Prével, J. L. Vialle, and M. Broyer, *Phys. Rev. B* **60**, 16 151 (1999).
- <sup>32</sup>M. Pellarin, B. Baguenard, M. Broyer, J. Lermé, J. L. Vialle, and A. Perez, *J. Chem. Phys.* **98**, 944 (1993).
- <sup>33</sup>A. Liebsch, *Phys. Rev. B* **48**, 11 317 (1993).
- <sup>34</sup>V. V. Krésin, *Phys. Rev. B* **51**, 1844 (1995).
- <sup>35</sup>K. J. Taylor, C. L. Pettiette-Hall, O. Cheshnovsky, and R. E. Smalley, *J. Chem. Phys.* **96**, 3319 (1992).
- <sup>36</sup>D. J. Bergman, *Phys. Rep.* **43**, 377 (1978).
- <sup>37</sup>D. J. Bergman, *Ann. Phys.* **138**, 78 (1982).
- <sup>38</sup>D. J. Bergman and D. Stroud, *Solid State Physics* (Academic Press, London, 1992).
- <sup>39</sup>J. C. Maxwell-Garnett, *Philos. Trans. R. Soc. London* **203**, 385 (1906).
- <sup>40</sup>D. A. G. Bruggeman, *Ann. Phys. (Leipzig)* **24**, 636 (1935).
- <sup>41</sup>W. F. J. Brown, *J. Chem. Phys.* **23**, 1514 (1955).
- <sup>42</sup>L. D. Landau, E. M. Lifshitz, and L. P. Pitaevskii, *Electrodynamics of Continuous Media* (Pergamon Press, Oxford, 1984).
- <sup>43</sup>E. D. Palik, *Handbook of Optical Constants of Solids* (Academic Press, New York, 1985/1991).
- <sup>44</sup>For instance the Bruggeman formula, that can be generalized for any number of components, was involved for calculating the dielectric constant of amorphous silicon-carbon alloys (the various components are ten individual Si- and C- centered tetrahedra).
- <sup>45</sup>K. Mui and F. W. Smith, *Phys. Rev. B* **35**, 8080 (1987).
- <sup>46</sup>In Fig. 4(b) the theoretical peak maxima for pure silver and gold clusters differ very slightly from those previously reported in the range  $N < 440$  (see Ref. 13). These tiny differences result, on the one hand from the use of the new formalism, on the other hand from the different value assumed for the width of the bound-bound particle-hole excitations for calculating the free response ( $2\delta = 200$  meV instead of 60 meV. As indicated in Ref. 13, the size-dependent fragmented pattern of the spectrum was smoothed with a Gaussian curve to estimate the location of the Mie resonance). Moreover, for solving the integral equation for the frequency-dependent density-density correlation function of large clusters, a very fine radial grid spacing was used in order to ensure maximum accuracy.